34th Annual International Conference of the IEEE EMBS
San Diego, California USA, 28 August - 1 September, 2012

Simulations and visualizations for interpretation of brain microdialysis data during deep brain stimulation

Elin Diczfalusy, Nil Dizdar, Peter Zsigmond, Anita Kullman, Dan Loyd, Karin Wårdell

Abstract—**Microdialysis of the basal ganglia was used in parallel to deep brain stimulation (DBS) for patients with Parkinson's disease. The aim of this study was to patient-specifically simulate and visualize the maximum tissue volume of influence (TVI_{max}) for each microdialysis catheter and the electric field generated around each DBS electrode. The finite element method (FEM) was used for the simulations. The method allowed mapping of the anatomical origin of the microdialysis data and the electric stimulation for each patient. It was seen that the sampling and stimulation targets differed among the patients, and the results will therefore be used in the future interpretation of the biochemical data.**

I. Introduction

Deep brain stimulation (DBS) is a technique commonly used for relief of movement disorders by electrical stimulation of deep brain structures [1]. The mechanisms behind DBS are still partly unknown [2], [3], and mathematical models have been widely used in order to predict how different electrical parameters influence the electric potential distribution around the DBS electrodes [4] - [10]. To further increase the understanding of the clinical outcome of DBS, brain microdialysis [11] can be used for biochemical sampling of neurotransmitters in the basal ganglia in parallel to the electric stimulation [12], [13].

At Linköping University Hospital, microdialysis has been used post-operatively in parallel to DBS for four patients with Parkinson´s disease, to monitor the behaviour of neuroactive substances such as dopamine (to be published). In order to compare the obtained data between the patients, it is suitable to map the sampling volume of each microdialysis catheter as well as the spread of the electric stimulation. Therefore, the aim of this study was to patient-specifically simulate and visualize the electric field around each DBS electrode [8] and the maximum tissue volume of influence (TVI_{max}) for each microdialysis catheter [14], using the finite element method (FEM). In this way, the biochemical data to be evaluated can be patient-specifically interpreted in relation to anatomical targets as well as to the spatial distribution of the electric fields generated during DBS.

Manuscript submitted February 21, 2012. The study was supported by the Swedish Governmental Agency for Innovation Systems (Vinnova), Swedish Foundation for Strategic Research (SSF), Swedish Research Council (VR) (Group grant no. 311-2006-7661), Research Foundation of the County Council of Östergötland, Medical Research Council of Southeast Sweden and Linköping University´s Foundation for Parkinson's Research.

E. Diczfalusy (corresponding author) and K. Wårdell are at the Department of Biomedical Engineering, Linköping University, Sweden (phone: +46-13-286746; e-mail: elin.diczfalusy@ liu.se).

N. Dizdar, P. Zsigmond and A. Kullman are at the Department of Clinical and Experimental Medicine, Linköping University, Sweden.

N. Dizdar is also at the Department of Neurology, Linköping University Hospital, Sweden.

P. Zsigmond is also at the Department of Neurosurgery, Linköping University Hospital, Sweden.

D. Loyd is at the Department of Management and Engineering, Linköping University, Sweden.

II. Materials and Methods

A. Patient data

Four patients (aged 56 ± 8) referred for bilateral implantation of DBS electrodes in the subthalamic nucleus (STN), were included in the study. In addition to the DBS electrodes (Model 3389 DBS™ Lead, Medtronics Inc. USA), three microdialysis catheters (10 mm length, 0.4 mm diameter; CMA65, CMA Microdialysis AB, Sweden) were stereotactically implanted in the putamen (right side) and the globus pallidus interna (GPi, left and right side). The patients gave informed written consent for participation in the study (Ethically approved by the Regional Ethics Committee at Linköping University, No. 51-04). Stereotactic imaging (1.5 T MRI-scanner, Philips Intera, The Netherlands) was performed after placement of the Leksell® Stereotactic System (model G, Elekta Instrument AB, Sweden). A stereotactic CT (GE Lightspeed Ultra, GE Healthcare, UK) was done directly after the implantations. Each patient was then referred to the neuro-intensive care unit where collection of biochemical samples was initiated. The microdialysis monitoring is a part of an ongoing study, and the results will be presented in a separate paper.

B. Patient-specific FEM simulations

1) Model setup: A three-dimensional patient-specific FEM model was set up for each patient. First, a brain tissue model was created, based on the patient's preoperative MRI images. Each tissue model included the basal ganglia and part of the midbrain. Intensity-based segmentation of the preoperative MRI was used for identification and electric conductivity classification of each voxel in the tissue model, since electrical properties differ between tissue types [15]. Next, two DBS electrode models and three microdialysis catheter models were created, based on the real dimensions, and positioned in each brain tissue model. The postoperative CT images acted as base for the positioning. A software tool (ELMA1.0) developed in MatLab 7.6 (The MathWorks, USA) was used for the classification of electric conductivity

and for positioning of the electrode and catheter models in the brain tissue model. An overview of the process is seen in Fig 1. For further details on how the models were set up, see [8], [14] and [16].

2) Governing equations: The equation for steady currents [17] was used for calculation of the distribution of the electric potential in the vicinity of the DBS electrodes:

$$\nabla \cdot \vec{J} = -\nabla \cdot [\sigma \nabla V] = 0 \qquad (1)$$

$\vec{J}$ is the current density (A m^{-2}), σ is the electrical conductivity (S m^{-1}), and V the electric potential (V).

For calculation of the TVI_{max}, a modified version of Fick´s diffusion law [14], [18], [19] was used:

$$\frac{\partial C}{\partial t} = \frac{D}{\lambda^2} \nabla^2 C - kC \qquad (2)$$

C = C(x,y,z,t) (nmol/litre) is the volume averaged analyte concentration, D is the analyte-specific diffusion coefficient in solution (m^2 s^{-1}), λ represents tissue tortuosity and k represents the analyte loss from the extracellular space (s^{-1}).

3) Simulations: The simulations were performed in a three-dimensional Cartesian co-ordinate system, using a FEM software (COMSOL Multiphysics 3.5, COMSOL AB, Stockholm, Sweden). The boundary and initial conditions are summarized in Fig 2, shown in an axi-symmetric co-ordinate system. The DBS electric potential was patient-specifically set according to the clinical parameters (Table I). D was set according to the substance of interest, in this case dopamine ($D = 7.5 \cdot 10^{-10}$ m^2 s^{-1} [20]). λ was set to 1.59 and k was set to 0.065 s^{-1}, intended to represent average values for the tissue and analyte of interest [19].

TABLE I
CLINICALLY EFFECTIVE DBS PARAMETERS

Patient	Active contacts	DBS stimulation parameters	Mean radius of simulated electric field isosurface
1	1-, 2-; 5-, 6-	1.5 V, 60 µs, 130 Hz	1.9 mm
2	1-, 2-; 5-, 6-	2.0 V, 60 µs, 130 Hz	2,4 mm
3	1-, 2-; 5-, 6-	2.0 V, 60 µs, 130 Hz	2.4 mm
4	1-, 2-; 5-, 6-	2.0 V, 60 µs, 130 Hz	2.3 mm

C. Visualization

The simulated electric fields and the TVI_{max} for each catheter were patient-specifically visualized in relation to the preoperative MRI images. An isolevel at 0.2 V mm^{-1} [5] was used to visualize the electric field, while the TVI_{max} was visualized with an isolevel at ($c_0 + 0.01c_b$) nmol/litre [14]. c_b is the analyte concentration at the catheter boundary (Fig 2).

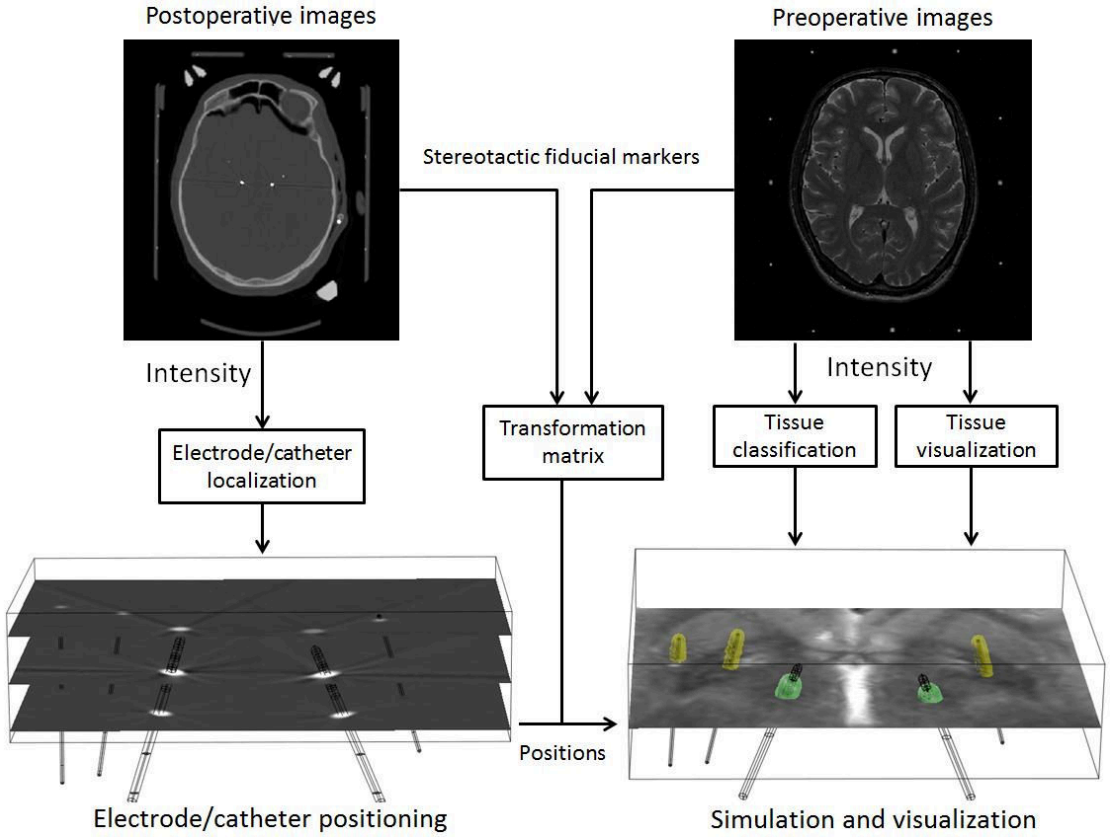

Figure 1. Overview of the FEM simulation process. The preoperative images are used to create a brain tissue model, including tissue segmentation, classification and visualization. The postoperative images are used to position electrode and catheter models correctly in the brain tissue model, based on image artifacts originating from the electrodes and catheters. Indicator box fiducial markers from the stereotactic system were used as landmarks.

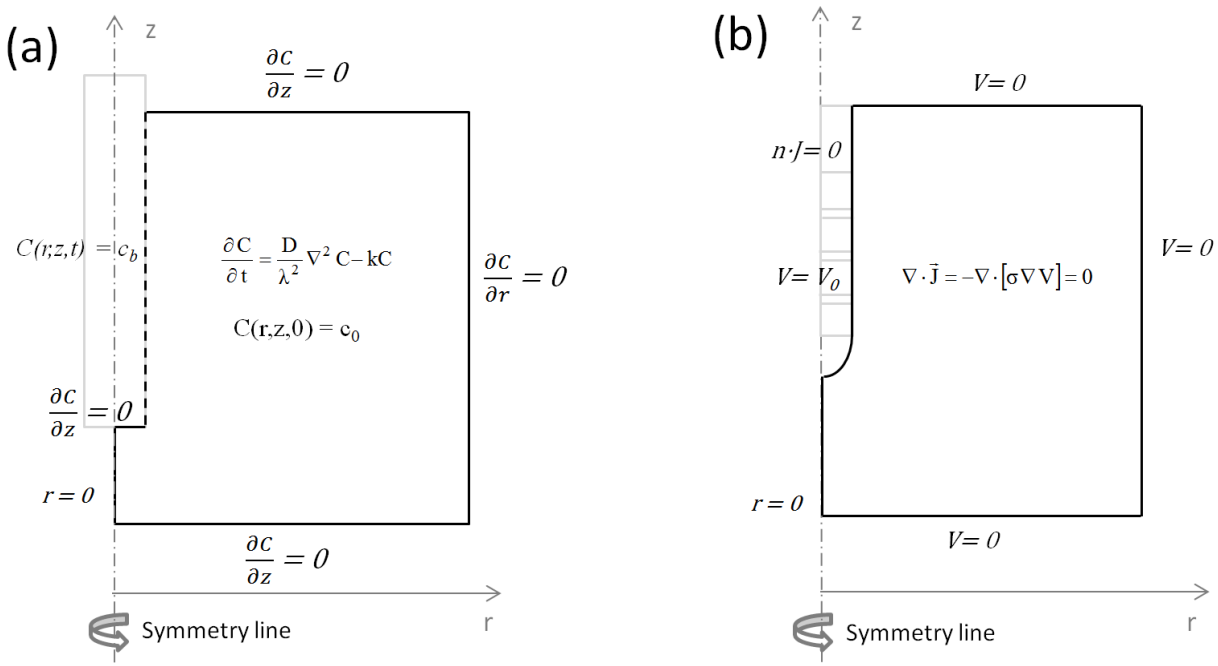

Figure 2. Initial and boundary conditions for the simulation of the TVI_{max} (a) and the DBS electric field (b), here shown in an axi-symmetric co-ordinate system. In (a), C is the analyte concentration (nmol/litre), D is the analyte diffusion coefficient ($m^2\ s^{-1}$), λ is the tissue tortuosity, k is the clearance constant (s^{-1}), c_0 is the initial analyte concentration in the tissue, c_b is the analyte concentration at the catheter boundary and r_c is the catheter radius. In (b), $\vec{J}$ is the current density ($A\ m^{-2}$), V is the electric potential (V) and σ is the tissue conductivity ($S\ m^{-1}$). V_0 is the electric potential at the active contact(s).

III. Results

Fig 3 shows the simulated electric fields and TVI_{max} in relation to axial MRI slices for the four patients. The mean radius of each electric field isolevel is included in Table I, and the cross-sectional radius of each TVI_{max} is 0.75 mm. Closer examination shows that the electric stimulation is centered around the dorsomedial/posterior STN for patient 1-3, while the substantia nigra is the main stimulation target for patient 4. The microdialysis catheters and their associated TVI_{max} are positioned at the targets aimed at (left GPi, right GPi, right putamen) for patient 1 and 3. For patient 2, the data from the right GPi is possibly influenced by the right globus pallidus externa (GPe). For patient 4, one catheter is located in the right putamen, another one in the right GPe and the third in the substantia nigra.

IV. Conclusions

In this study, simulations and visualizations were made to enable patient-specific mapping of the DBS electric fields and the microdialysis catheters with their associated TVI_{max} in relation to anatomical structures. It is seen that there are differences among the patients regarding the microdialysis target structures as well as the extension of the DBS electric fields, which may affect the biochemical measurements. The results of this study will therefore be used as a foundation in the future interpretation of the obtained biochemical data, to verify whether the catheter positions and generated electric fields are consistent among the patients, and whether this influences the clinical outcome.

The TVI_{max} is here simulated using λ and k values meant to represent the average brain tissue. The radius of the TVI_{max} for the current D value may, however, increase by up to 0.25 mm (28%) when λ and k vary within physiologically relevant intervals [14]. This should be taken into account when the data is to be evaluated.

An isolevel at 0.2 V mm^{-1} [5], [8], [21] is used for visualization of the DBS electric fields. The volume within this isolevel is not to be considered the tissue volume affected by DBS; rather, its radius (Table I) lies within the estimated volume of influence for standard DBS parameters [10] and it is therefore used here for a rough comparison between the patients. Other parameters, such as the commonly used neuronal activation function [4], [22], can be derived from the calculated electric field in order to draw further conclusions about the electric stimulation on a neuronal level.

Acknowledgment

The authors would like to thank Johan Richter, MD, and the staff at Neurosurgical Department of Linköping University Hospital for skillful help during the measurements. The authors would also like to thank Mattias Åström, PhD, at Sapiens Steering Brain Stimulation, (Eindhoven, The Netherlands) for valuable discussions concerning the simulations.

References

[1] Benabid, A.L., *Deep brain stimulation for Parkinson's disease.* Curr Opin Neurobiol, 2003. **13**(6): p. 696-706.

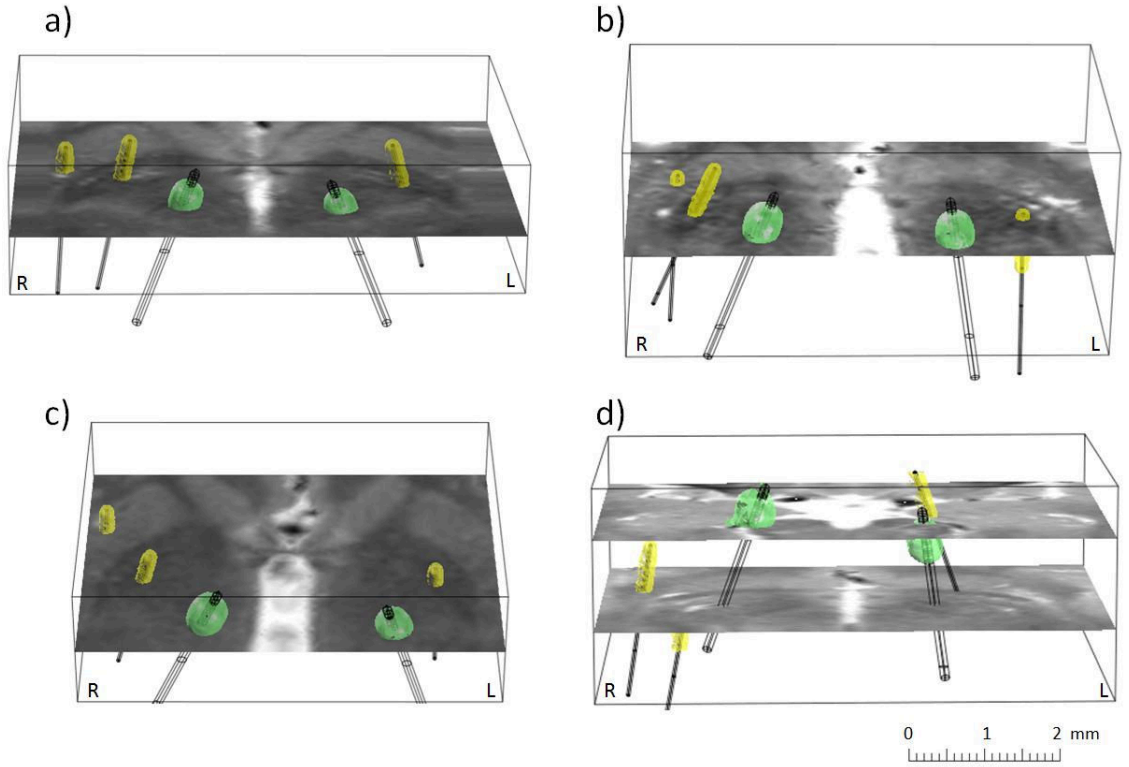

Figure 3. Visualization of the simulated electric field around each DBS electrode (isolevel at 0.2 V/mm) and the TVI_{max} for each microdialysis catheter (isolevel at $0.01c_b$, where c_b is the analyte concentration at the catheter boundary), shown together with axial MRI slices for each patient. a) Patient 1, b) Patient 2, c) Patient 3, d) Patient 4.

[2] Johnson, M.D., S. Miocinovic, C.C. McIntyre, and J.L. Vitek, *Mechanisms and targets of deep brain stimulation in movement disorders.* Neurotherapeutics, 2008. **5**(2): p. 294-308.

[3] Montgomery, E.B., Jr. and J.T. Gale, *Mechanisms of action of deep brain stimulation(DBS).* Neurosci Biobehav Rev, 2008. **32**(3): p. 388-407.

[4] Butson, C.R., S.E. Cooper, J.M. Henderson, and C.C. McIntyre, *Patient-specific analysis of the volume of tissue activated during deep brain stimulation.* Neuroimage, 2007. **34**(2): p. 661-70.

[5] Hemm, S., G. Mennessier, N. Vayssiere, L. Cif, H. El Fertit, and P. Coubes, *Deep brain stimulation in movement disorders: stereotactic coregistration of two-dimensional electrical field modeling and magnetic resonance imaging.* J Neurosurg, 2005. **103**(6): p. 949-55.

[6] McIntyre, C.C., S. Mori, D.L. Sherman, N.V. Thakor, and J.L. Vitek, *Electric field and stimulating influence generated by deep brain stimulation of the subthalamic nucleus.* Clinical neurophysiology : official journal of the International Federation of Clinical Neurophysiology, 2004. **115**(3): p. 589-95.

[7] Vasques, X., L. Cif, O. Hess, S. Gavarini, G. Mennessier, and P. Coubes, *Stereotactic model of the electrical distribution within the internal globus pallidus during deep brain stimulation.* Journal of computational neuroscience, 2009. **26**(1): p. 109-18.

[8] Astrom, M., L.U. Zrinzo, S. Tisch, E. Tripoliti, M.I. Hariz, and K. Wardell, *Method for patient-specific finite element modeling and simulation of deep brain stimulation.* Med Biol Eng Comput, 2009. **47**(1): p. 21-8.

[9] Bayford, R.T., A.; Liu, X., *Dynamic modelling of electrical current distribution in the deep structure of the brain.* Medical Applications of Signal Processing, 2005 (Ref. No. 2005-1119), 2005: p. 131- 134.

[10] Kuncel, A.M., S.E. Cooper, and W.M. Grill, *A method to estimate the spatial extent of activation in thalamic deep brain stimulation.* Clinical neurophysiology : official journal of the International Federation of Clinical Neurophysiology, 2008. **119**(9): p. 2148-58.

[11] Chefer, V.I., A.C. Thompson, A. Zapata, and T.S. Shippenberg, *Overview of brain microdialysis.* Curr Protoc Neurosci, 2009. **Chapter 7**: p. 7.1.1-7.1.22.

[12] Galati, S., P. Mazzone, E. Fedele, A. Pisani, A. Peppe, M. Pierantozzi, L. Brusa, D. Tropepi, V. Moschella, M. Raiteri, et al., *Biochemical and electrophysiological changes of substantia nigra pars reticulata driven by subthalamic stimulation in patients with Parkinson's disease.* Eur J Neurosci, 2006. **23**(11): p. 2923-8.

[13] Stefani, A., E. Fedele, S. Galati, M. Raiteri, O. Pepicelli, L. Brusa, M. Pierantozzi, A. Peppe, A. Pisani, G. Gattoni, et al., *Deep brain stimulation in Parkinson's disease patients: biochemical evidence.* J Neural Transm Suppl, 2006 (70): p. 401-8.

[14] Diczfalusy, E., P. Zsigmond, N. Dizdar, A. Kullman, D. Loyd, and K. Wardell, *A model for simulation and patient-specific visualization of the tissue volume of influence during brain microdialysis.* Medical & biological engineering & computing, 2011. **49**(12): p. 1459-69.

[15] Aundreccetti, D., R. Fossi, and C. Petrucci, *Dielectric properties of body tissue.* Italian National Research Council, Institute for Applied Physics, Florence, Italy, 2005.

[16] Wårdell, K., E. Diczfalusy, and M. Åström, *Patient-Specific Modeling and Simulation of Deep Brain Stimulation*, in *Studies in Mechanobiology, Tissue Engineering and Biomaterials,* 2011, Springer-Verlag: Berlin Heidenberg.

[17] Cheng, D.K., *Field and Wave Electromagnetics*. Vol. ISBN 0-201-52820-7. 1989: Addison-Wesley Publishing Company Inc.

[18] Nicholson, C., *Diffusion and related transport mechanisms in brain tissue.* Reports on Progress in Physics, 2001. **64**(7): p. 815-884.

[19] Sykova, E. and C. Nicholson, *Diffusion in brain extracellular space.* Physiological Reviews, 2008. **88**(4): p. 1277-1340.

[20] Rice, M.E., G.A. Gerhardt, P.M. Hierl, G. Nagy, and R.N. Adams, *Diffusion coefficients of neurotransmitters and their metabolites in brain extracellular fluid space.* Neuroscience, 1985. **15**(3): p. 891-902.

[21] Astrom, M., E. Tripoliti, M.I. Hariz, L. Zrinzo, I. Martinez-Torres, P. Limousin, and K Wardell, *Patient-specific model-based investigation of speech intelligibility and movement during deep brain stimulation,* Stereotact Funct Neurosurg, 2010. **88**(4): p 224-33.

[22] Holsheimer, J., *Principles of Neurostimulation*, in *Electric stimulation and the relief of pain*, B.A. Simpson, Editor 2003, Elsevier Health Sciences. p. 17-36.